STEM CELLS TRANSLATIONAL MEDICINE®

CANCER STEM CELLS

# Targeting Cancer Stem Cell Plasticity Through Modulation of Epidermal Growth Factor and Insulin-Like Growth Factor Receptor Signaling in Head and Neck Squamous Cell Cancer

HUI SUN LEONG,[a] FUI TEEN CHONG,[a] PUI HOON SEW,[a] DAWN P. LAU,[a] BERNICE H. WONG,[b] BIN-TEAN TEH,[b] DANIEL S.W. TAN,[a,c] N. GOPALAKRISHNA IYER[a,d]

**Key Words.** Epidermal growth factor receptor • Insulin-like growth factor-1 receptor • Aldehyde dehydrogenase • Head and neck squamous cell cancer • Cancer stem cell

[a]Cancer Therapeutics Research Laboratory, [b]Laboratory of Cancer Epigenome, [c]Department of Medical Oncology, and [d]Department of Surgical Oncology, National Cancer Centre Singapore, Singapore

Correspondence: N. Gopalakrishna Iyer, M.D., Ph.D., Cancer Therapeutics Research Laboratory, National Cancer Centre Singapore, 11 Hospital Drive, Singapore 169610. Telephone: 65-64-36-8294; E-Mail: gopaliyer@yahoo.com; or Daniel S.W. Tan, M.D., Cancer Therapeutics Research Laboratory, National Cancer Centre Singapore, 11 Hospital Drive, Singapore 169610. Telephone: 65-6436-8547; E-Mail: Daniel.tan.s.w@nccs.com.sg

Received December 10, 2013; accepted for publication May 21, 2014; first published online in SCTM *Express* July 14, 2014.


1066-5099/2014/$20.00/0

http://dx.doi.org/10.5966/sctm.2013-0214

## ABSTRACT

**Emerging data suggest that cancer stem cells (CSCs) exist in equilibrium with differentiated cells and that stochastic transitions between these states can account for tumor heterogeneity and drug resistance. The aim of this study was to establish an in vitro system that recapitulates stem cell plasticity in head and neck squamous cell cancers (HNSCCs) and identify the factors that play a role in the maintenance and repopulation of CSCs. Tumor spheres were established using patient-derived cell lines via anchorage-independent cell culture techniques. These tumor spheres were found to have higher aldehyde dehydrogenase (ALD) cell fractions and increased expression of Kruppel-like factor 4, SRY (sex determining region Y)-box 2, and Nanog and were resistant to $\gamma$-radiation, 5-fluorouracil, cisplatin, and etoposide treatment compared with monolayer culture cells. Monolayer cultures were subject to single cell cloning to generate clones with high and low ALD fractions. $ALD^{High}$ clones showed higher expression of stem cell and epithelial-mesenchymal transition markers compared with $ALD^{Low}$ clones. ALD fractions, representing stem cell fractions, fluctuated with serial passaging, equilibrating at a level specific to each cell line, and could be augmented by the addition of epidermal growth factor (EGF) and/or insulin. $ALD^{High}$ clones showed increased EGF receptor (EGFR) and insulin-like growth factor-1 receptor (IGF-1R) phosphorylation, with increased activation of downstream pathways compared with $ALD^{Low}$ clones. Importantly, blocking these pathways using specific inhibitors against EGFR and IGF-1R reduced stem cell fractions drastically. Taken together, these results show that HNSCC CSCs exhibit plasticity, with the maintenance of the stem cell fraction dependent on the EGFR and IGF-1R pathways and potentially amenable to targeted therapeutics.** STEM CELLS TRANSLATIONAL MEDICINE *2014;3:1055–1065*

## INTRODUCTION

Head and neck squamous cell cancers (HNSCCs) account for approximately 650,000 new cases and 350,000 deaths annually worldwide [1, 2]. Most patients with locoregional disease will succumb to tumor recurrence, due to resistance to conventional treatment strategies, including radiation and cytotoxic chemotherapy. In the advanced stage, prognosis is poor, with a median survival of 6–9 months. Apart from cetuximab, no targeted treatment approaches are currently approved, and conventional platinum-based two-drug combination cytotoxic chemotherapy affords response rates of only 15%–30% [3].

Treatment resistance can be accounted for by the persistence of aggressive tumor subclones. Mounting evidence has shown that heterogeneous cell subpopulations exist within solid tumors and that a subset of these cells has the capacity for self-renewal and display stem cell-like properties (cancer stem cells [CSCs]), including chemotherapy- and radiation-resistance, increased invasiveness, epithelial-mesenchymal transition (EMT), and a propensity for metastases [4–6]. Furthermore, these subpopulations have been characterized from several tumor types, including HNSCCs, using cell surface markers (e.g., CD133, CD44, CD166), biochemical assays (e.g., aldehyde dehydrogenase activity), and cell phenotype (e.g., an ability to form spheres, an ability to extrude Hoechst dyes) [7–14]. The presence of CSCs or a stem cell-like phenotype is an important predictor of treatment failure and disease recurrence, and new treatment strategies are urgently needed [15–17].

Recent studies have challenged the notion of whether cancer stem cells follow a hierarchical propagation through asymmetric replication [4, 18] and suggested that the balance between CSCs and differentiated cells results from stochastic

**Table 1.** Patient characteristics for patient-derived primary cell lines[a]

| Cell line | Sex/age (yr) | Primary site | Type | Treatment | Outcome |
|---|---|---|---|---|---|
| NCC-HN1 | F/25 | Tongue | Recurrence | Surgery, palliative chemotherapy | Distant metastases, died of disease 5 mo after diagnosis of recurrence |
| NCC-HN19 | M/48 | Tongue | Primary | Surgery, adjuvant chemoradiation therapy | Distant metastases, died of disease 7 mo after initial diagnosis |
| NCC-HN26 | M/60 | Hard palate | Primary | Surgery, adjuvant chemoradiation therapy | Alive 3 yr without disease |

[a]All cell lines were established from tumors that were histologically proven to be squamous cell carcinoma and obtained from surgical material derived from lymph node metastases.
Abbreviations: F, female; M, male.

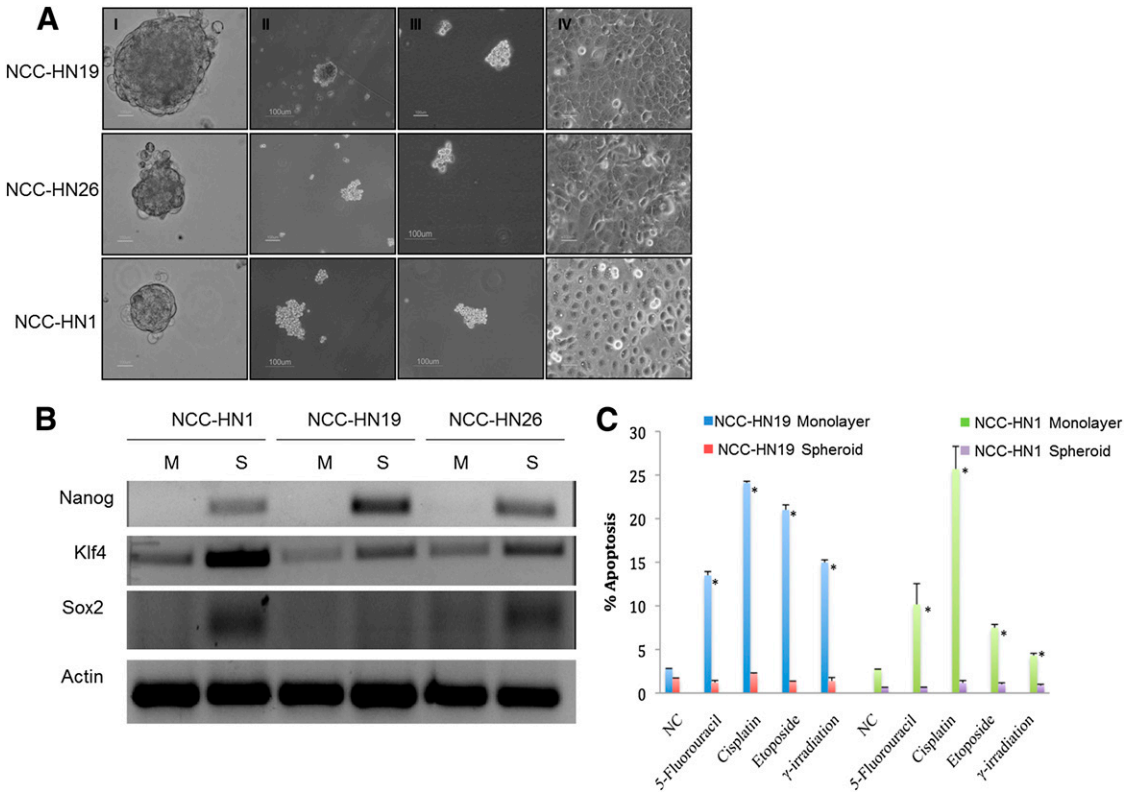


**Figure 1.** Tumor spheres generated from HNSCC cells demonstrated CSC properties. **(A):** Phase-contrast microscopy images of HNSCC primary cell lines are shown. Panels I–III show first, second, and third generation sphere cultures formed after re-plating as described. Panel IV shows adherent cells grown as monolayer cultures after re-plating from tertiary sphere culture. Scale bar represents 100 $\mu$m. **(B):** RT-PCR shows increased expression of stem cell markers Nanog, Klf4, and Sox2 in tumor spheres compared to monolayer cultures. **(C):** Graph showing percentage apoptosis after treatment with 5-fluorouracil (3 $\mu$M for NCC-HN19, 0.1 $\mu$M for NCC-HN1), cisplatin (3.5 $\mu$M for NCC-HN19, 3.0 $\mu$M for NCC-HN1), etoposide (2 $\mu$M for NCC-HN19, 6 $\mu$M for NCC-HN1), or $\gamma$-irradiation (2 Gy for NCC-HN19, 4 Gy for NCC-HN1). These show that tumor spheres are more resistant compared to monolayer cultures All drug and irradiation treatments were run in three independent experiments, and standard deviation is indicated ($*$, $p < .05$). Abbreviations: M, monolayer; NC, negative control (untreated); S, spheroid.

transitions between distinct tumor states [19, 20]. From these data, we hypothesized that this process is dynamic and bidirectional, such that CSCs and progenitors exist in a contextually regulated equilibrium, with intrinsic control mechanisms driven by the tumor cells and extrinsic influences from the tumor microenvironment. Several studies have shown that factors in the tumor microenvironment involved in this process include interleukin-6, chemokine (C-X-C motif) ligand 7, and transforming growth factor-$\beta$ in breast cancer and hepatocyte growth factor in colon cancer [21–23].

We describe the establishment of patient-derived HNSCC cell lines, in which a dynamic subpopulation demonstrates stem cell markers and resistance to conventional chemotherapy. Our data show that epidermal growth factor (EGF) receptor (EGFR) and insulin-like growth factor-1 (IGF-1) receptor (IGF-1R) signaling play a critical role in maintaining this stem cell phenotype and that dual inhibition is a plausible therapeutic strategy for head and neck squamous cell carcinoma.

## Materials and Methods

### Tumor Specimens and Primary Tumor/Sphere Cultures

After obtaining informed consent, tumor samples classified as HNSCC using the World Health Organization criteria were

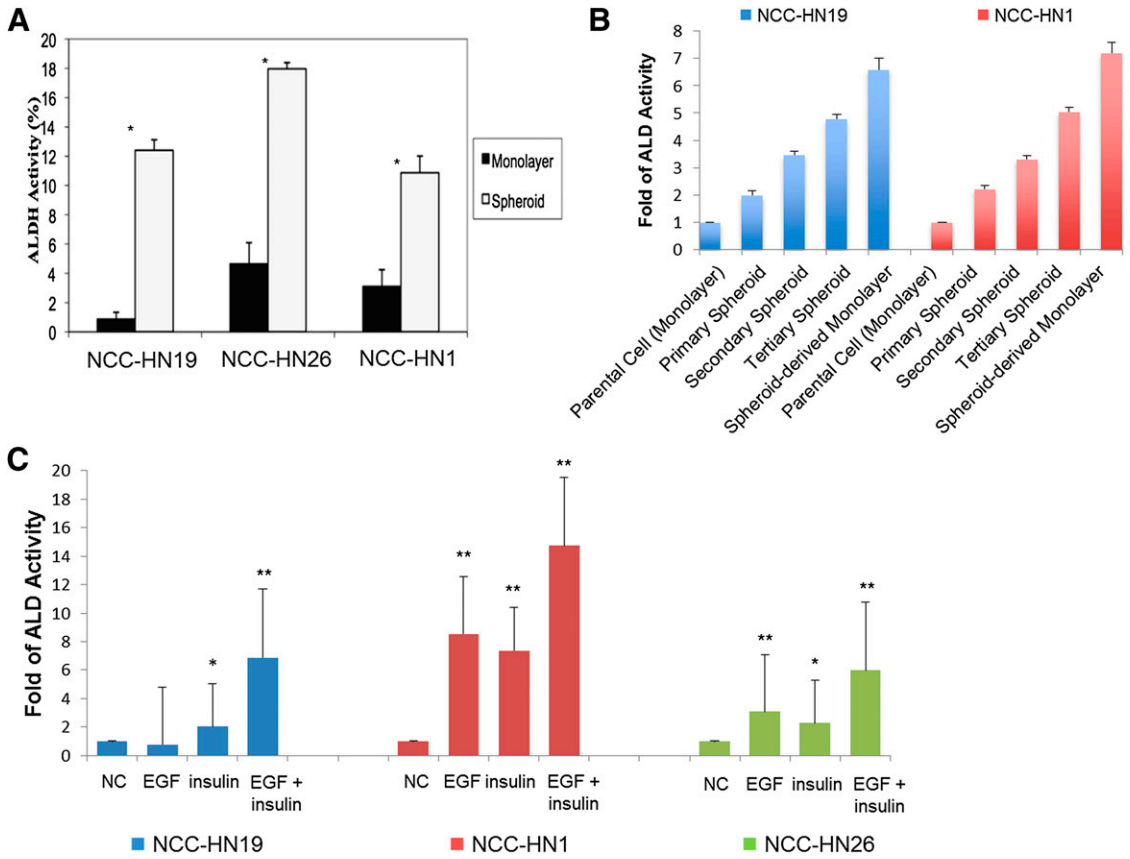


**Figure 2.** ALD-positive (ALD+) cells were concentrated in HNSCC tumor spheres and after treatment with growth factors. **(A):** Graph showing percentage of ALD+ cells in monolayer and tumor sphere cultures. Error bars indicate one standard deviation obtained from three independent experiments (*, $p < .05$). **(B):** Graph showing percentage of ALD+ cells in serial passages of first, second, and third generation tumor spheres, and subsequent monolayer culture of third generation spheroids, showing progressive concentration of the CSC population. **(C):** Graph showing percentage of ALD+ cells in monolayer cultures after addition of EGF and/or insulin, with increased levels of ALD+ cells after growth factor addition. ALD levels were normalized to untreated controls and standard deviation is indicated (*, $p < .05$, **, $p < .01$, ***, $p < .001$). Abbreviations: ALD/ALDH, aldehyde dehydrogenase; EGF, epidermal growth factor; NC, negative control (untreated).

obtained from patients undergoing surgical treatment at the National Cancer Centre Singapore in accordance with approval from the Singhealth Centralized institutional review board that was current at the time of the experiments (CIRB 2007/441/B). Within 1–3 hours after surgical removal, the tumors were washed and enzymatically dissociated with collagenase (Roche, Hvidovre, Denmark, http://www.roche.com) into single cells. Red blood cells were removed by differential centrifugation. Tumor cells were cultured in Roswell Park Memorial Institute (RPMI) medium (Sigma-Aldrich, St. Louis, MO, http://www.sigmaaldrich.com) supplemented with 10% fetal bovine serum (FBS) (HyClone, Thermo Scientific, Inc., Fremont, CA, http://www.thermoscientific.com) and 1% penicillin-streptomycin (Gibco, Invitrogen, Carlsbad, CA, http://www.invitrogen.com) in a humidified atmosphere of 5% $CO_2$ at 37°C. For sphere culture, cell lines were grown with the following media: Dulbecco's modified Eagle medium/Ham F12 (1:1) (Gibco), supplemented with 5% bovine serum albumin (Gibco), 2% FBS (Hyclone), 10 mM HEPES, B27 (Gibco), 20 ng/ml EGF, 20 ng/ml basic fibroblast growth factor (bFGF) (Gene-Ethics, Carlton, Victoria, Australia, http://www.geneethics.org), 10 $\mu$g/ml insulin (Gibco), and 10 ng/ml heparin (Gibco). After trypsinization, the cells were confirmed to be single cells by passing them through a 75-$\mu$M cell strainer. Fresh media were replenished every 3 days. Tumor spheres were formed in 48–72 hours and were ready for subsequent experiments 4–9 days after plating. Details of the cell line origin are outlined in subsequent sections. In all cases, cell lines were obtained at the primary surgery before any treatment. Cell line identity was authenticated by targeted sequencing of the line and original primary tumor they were derived from to determine identical single nucleotide polymorphisms (data not shown).

## Drug Treatment and Western Blots

Tissue culture conditions and drug treatments were performed as described. Gefitinib was obtained from BioVision (Milpitas, CA, http://www.biovision.com), and NVP-AEW541 was purchased from Cayman Chemicals (Ann Arbor, MI, http://www.caymanchem.com). 5-Fluorouracil, cisplatin, and etoposide were obtained from Sigma-Aldrich. Western blots were performed as previously described [24]. The antibodies used were as follows: rabbit polyclonal antibodies to Oct-4, Bmi-1, Nanog, N-cadherin, E-cadherin, Slug, Snail, $\beta$-catenin, vimentin, claudin 1, IGF-1R, phospho-IGF-1R (Tyr 1135), EGFR, phospho-EGFR (Tyr 1068), HER-2, phospho-HER-2 (Tyr 1221/1222), HER-3, phospho-HER-3 (Tyr 1222), AKT, phospho-AKT (Ser 473), Erk 1/2, phospho-Er1/2 (Thr202/204), AMPK, phospho-AMPK (Thr 172),

 

**Table 2.** ALD+ fractions in subclones derived from NCC-HN1, NCC-HN19, and NCC-HN26 cell lines obtained by serial dilution

| Cell line and subclone | | ALD (%) | SD |
|---|---|---|---|
| NCC-HN1 | Clone 1[a] | 1.90 | 0.14 |
| | Clone 14 | 3.15 | 0.21 |
| | Clone 24[b] | 35.95 | 0.64 |
| | Clone 27 | 1.55 | 0.07 |
| | Clone 31 | 10.75 | 0.07 |
| | Clone 33[a] | 0.40 | 0.00 |
| | Clone 34 | 2.05 | 0.07 |
| | Clone 35 | 7.50 | 0.42 |
| | Clone 36 | 2.40 | 0.14 |
| | Clone 37 | 4.55 | 0.07 |
| | Clone 53 | 2.65 | 0.07 |
| | Clone 66 | 1.65 | 0.07 |
| | Clone 110 | 7.05 | 0.21 |
| | Clone 112 | 14.45 | 0.78 |
| | Clone 113[b] | 21.30 | 0.71 |
| NCC-HN19 | Clone 31 | 3.40 | 0.00 |
| | Clone 33 | 13.15 | 0.21 |
| | Clone 34 | 10.20 | 0.00 |
| | Clone 36 | 6.00 | 0.14 |
| | Clone 37 | 9.70 | 0.28 |
| | Clone 39[b] | 27.00 | 1.13 |
| | Clone 40 | 8.25 | 0.07 |
| | Clone 41[a] | 2.60 | 0.00 |
| | Clone 43[a] | 0.70 | 0.00 |
| | Clone 47 | 6.75 | 0.07 |
| | Clone 50 | 11.65 | 0.35 |
| | Clone 51[b] | 14.10 | 0.57 |
| | Clone 52 | 13.55 | 0.07 |
| | Clone 84 | 13.30 | 0.42 |
| | Clone 87 | 4.15 | 0.21 |
| | Clone 91 | 11.90 | 0.28 |
| NCC-HN26 | Clone 11 | 5.45 | 0.21 |
| | Clone 12[b] | 12.25 | 0.35 |
| | Clone 13 | 5.05 | 0.21 |
| | Clone 18 | 10.70 | 1.13 |
| | Clone 22 | 8.45 | 0.07 |
| | Clone 50 | 2.20 | 0.28 |
| | Clone 51 | 1.75 | 0.21 |
| | Clone 52 | 2.30 | 0.28 |
| | Clone 53[a] | 1.35 | 0.07 |
| | Clone 56[a] | 0.60 | 0.00 |
| | Clone 59 | 6.65 | 0.35 |
| | Clone 60 | 7.55 | 0.07 |
| | Clone 64 | 2.15 | 0.21 |
| | Clone 66 | 4.20 | 0.28 |
| | Clone 76 | 4.75 | 0.07 |
| | Clone 79[b] | 18.45 | 0.07 |

[a]$ALD^{Low}$ clones used for subsequent experiments.
[b]$ALD^{High}$ clones used for subsequent experiments.
Abbreviation: ALD, aldehyde dehydrogenase.

S6, phospho-S6 (Ser 235/236), phospho-Bad (Ser 112), p38, and phospho-p38 (Thr 180/Tyr 182) (Cell Signaling Technology, Danvers, MA, http://www.cellsignal.com), twist 1/2 (Santa Cruz Biotechnology Inc., Santa Cruz, CA, http://www.scbt.com), and mouse monoclonal antibody to Bad and goat polyclonal antibody to actin (Santa Cruz Biotechnology).

### ALDEFLUOR Assay and Flow Cytometric Analysis

Aldehyde dehydrogenase (ALD) activity from HNSCC cells was measured using the ALDEFLUOR assay kit (StemCell Technologies Inc., Vancouver, British Columbia, Canada) following the manufacturer's instructions and analyzed using fluorescent-activated cell sorting (FACS). In brief, trypsinized cells were resuspended in ALDEFLUOR assay buffer containing ALD substrate with a concentration of 1 M per $1 \times 10^6$ cells and incubated for 1 hour at 37°C. For every individual sample, an aliquot was treated with 30 $\mu$M diethylaminobenzaldehyde (DEAB), a specific ALD inhibitor, as a negative control. The cells were then FACS-sorted using a FACSAria or read out with FACSCanto II (BD Biosciences, San Jose, CA, http://www.bdbiosciences.com) and analyzed with FACSDiva software (BD Biosciences). Sorting gates were established using the ALDEFLUOR-stained cells treated with DEAB as negative controls. ALD-positive cells were classed as those emitting fluorescence greater than the DEAB-treated control cells. Cell viability was determined using 7AAD (BD Biosciences) staining during FACS analysis. For each assay, we analyzed the ALD fraction in 10,000 cells to obtain the percentage of cells positive for ALD.

### Isolation of $ALD^{High}$ and $ALD^{Low}$ Clones

Single cell suspensions obtained from serial dilution were plated in 96-well plates. Fresh media were replaced every 3 days until single cell clones appeared. Approximately 50 clones of HNSCC appeared 14 days after plating. Isolated clones were individually expanded in RPMI medium (Sigma-Aldrich) supplemented with 10% FBS and 1% penicillin-streptomycin (Gibco). The cells were analyzed with the ALDEFLUOR assay for ALD activity. For all Western blots shown, we used the clones with the extremes of ALD fractions to demonstrate the point. However, similar results were obtained with the unused clones, in which good (dose-dependent) correlation was found between the intensity of Western blots and the ALD fractions in the other clones. For drug assays, two clones were used per cell line for the $ALD^{High}$ and $ALD^{Low}$ cells.

### Apoptosis Analysis and Colony Formation Assays

The cells were harvested 48 hours after drug treatment and processed for propidium iodide staining for determination of sub-$G_1$ fractions, as previously described [24]. For colony forming assays, $ALD^{High}$ and $ALD^{Low}$ cells were plated onto 6-well plates at a density of 5,000 cells per well in RPMI medium supplemented with 10% FBS and 1% penicillin-streptomycin. The $ALD^{High}$ and $ALD^{Low}$ cells were treated with various cytotoxic drugs or $\gamma$-irradiation at the respective half-maximal inhibitory concentration dosage of their parental cell. The cells were then grown in standard culture conditions for 21 days with fresh media replaced every 3 days. The colonies were stained with crystal violet (0.25% wt/vol) (Sigma-Aldrich), and the clone numbers were counted using a stereomicroscope.

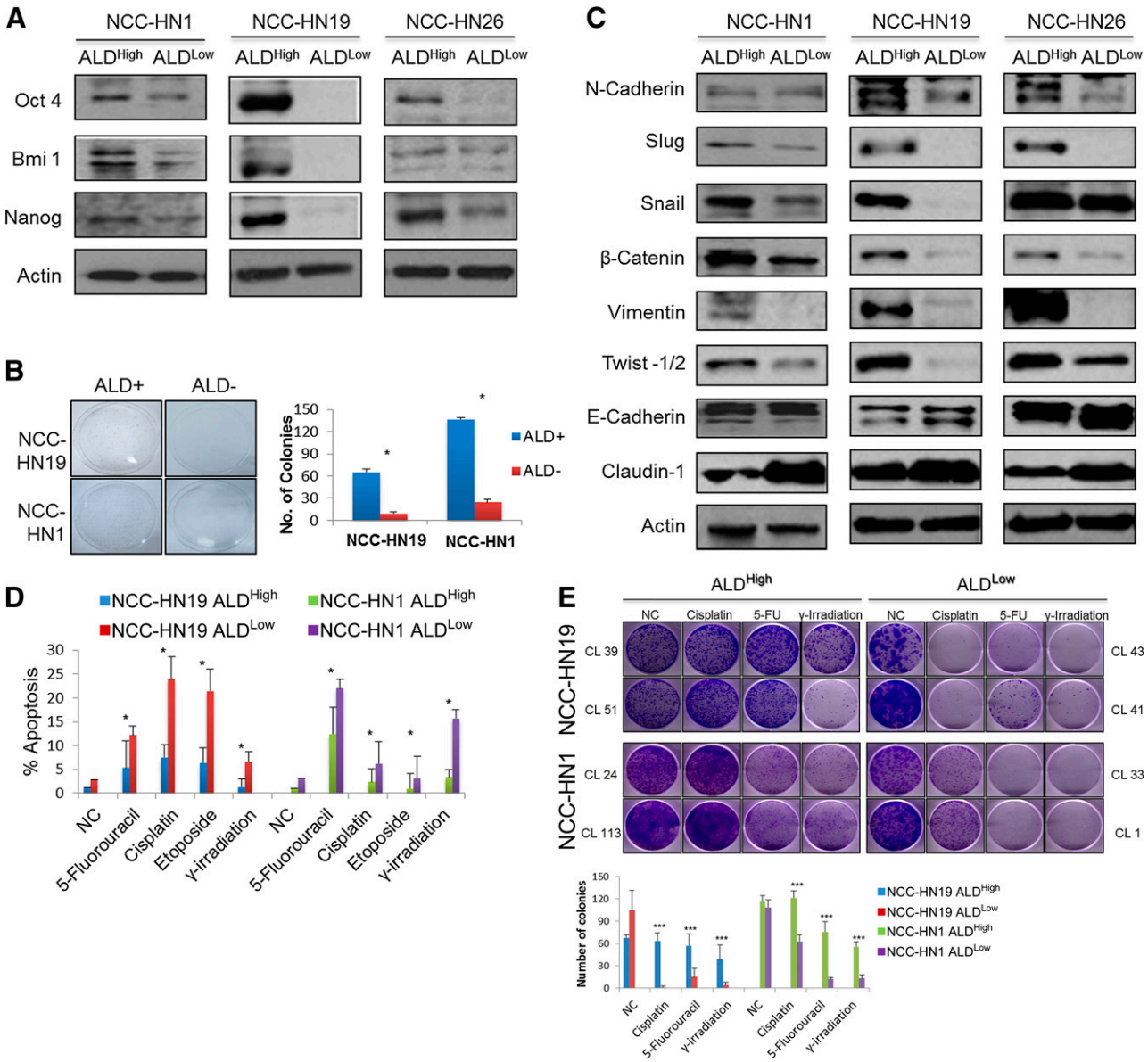


**Figure 3.** ALD+ cells have characteristicsof CSCs, show features of epithelial-mesenchymal transition and are resistant to cytoxic therapy. **(A):** Western blots showing that ALD$^{High}$ cells have higher expression of stem cell markers Oct4, Bmi1, Nanog, compared to ALD$^{Low}$ cells with actin loading control. **(B):** Plating assays and graph showing number of surviving colonies showing that ALD$^{High}$ cells demonstrated higher clonogenic capacity compared to ALD$^{Low}$ cells. In this experiment, ALD$^{High}$ and ALD$^{Low}$ cells were isolated by FACS sorting, plated at equal density and cultured for 21 days. Surviving cells were stained with crystal violet (∗, $p < .05$). **(C):** Western blots of E-M-T markers showing that ALD$^{High}$ cells show features of E-M-T compared to ALD$^{Low}$ cells. ALD$^{High}$ cells expressed more mesenchymal markers, N-Cadherin, Slug, Snail, b-Catenin, Vimentin, and Twist-½; whereas ALD$^{Low}$ cells expressed more of epithelial markers, E-Cadherin and Claudin-1. **(D):** Graph showing percentage apoptosis after treatment with various cytotoxic treatments. These show that ALD$^{High}$ clones are more resistant compared to ALD$^{Low}$ clones. All drug and irradiation treatments were run at $IC_{50}$ dose of their respective parental cell lines, and standard deviation from three independent experiments is indicated (∗, $p < .05$). **(E):** Plating assays and graph showing number of surviving colonies showing that ALD$^{High}$ cells are significantly more resistant to various cytotic drugs and γ-irradiation as compared to ALD$^{Low}$ cells. In this experiment, ALD$^{High}$ and ALD$^{Low}$ cells were plated at equal density, treated at $IC_{50}$ dose of their respective parental cell lines for 48 hours and cultured for 21 days. Surviving cells were stained with crystal violet and number of colonies were calculated, standard deviation from three independent experiments is indicated (∗∗∗, $p < .0001$). Western blots were performed on clones with the most extreme ALD fractions, so for ALD$^{High}$ cells NCC-HN1 Clone 24, NCC-HN19 Clone 39 and NCC-HN26 Clone 79 were used while for ALD$^{Low}$ cells NCC-HN1 Clone 33, NCC-HN19 Clone 43 and NCC-HN26 Clone 56 were used. For drug assays, two clones per cell line were used as indicated, and each cell line experiment was performed in triplicate, with data showing the average and standard deviation of these. Abbreviations: ALD, aldehyde dehydrogenase; ALD$^{High}$, clones with high ALD+ fraction; ALD$^{Low}$, clones with low ALD+ fraction; NC, negative control (untreated).

### Reverse Transcriptase-Polymerase Chain Reaction

Total RNA was extracted from monolayer and tumor spheres of NCC-HN1, NCC-HN19, and NCC-HN26 cell lines using the RNeasy kit (Qiagen, Valencia, CA, http://www.qiagen.com) according to the manufacturer's instructions. Reverse transcriptase-polymerase chain reaction (RT-PCR) was performed as previously described [24]. Reactions were performed in triplicate, with actin serving as the normalizing control. The primer sequences used were as follows:

 

Nanog forward, 5′-CAGTCTGGACACTGGCTGAATCCTT-3′; Nanog reverse, 5′-GCTGATTAGGCTCCAA CCATACTC-3′; KLF4 forward, 5′-ATCCTTCCTGCCCGATCAGATG-3; KLF4 reverse, 5′-GCCTTGAGATGGGAACTCTTTGTG-3′; Sox2 forward, 5′-AAAGAGAACACCAATCCCATCCAC-3′; Sox2 reverse, 5′-CTTTCCTCCAGATCTATACAAGGTCC-3′; Actin forward, 5′-TGTTTGAGACCTTCAACACC-3′; Actin reverse, 5′-AGGTAGTCAGTCAGGTCCCGGCC-5′.

### Statistical Analysis

Statistical analyses were performed using PASW statistics, version 18.0 (IBM Corp., Armonk, NY, http://www-01.ibm.com/software/analytics/spss/). Student's *t* test and the Mann-Whitney *U* test were used to compare the group means and the chi-square test was used to analyze the other factors.

## RESULTS

### HNSCC Patient-Derived Cell Lines Develop Tumor Spheres and Exhibit CSC Properties

Cell lines were established from patient-derived fresh tumor tissue, as described. All tumors were derived from cervical node metastases of HNSCC at the primary surgery before any other treatment. The patient details are summarized in Table 1. Genotyping was performed and confirmed that each cell line was genetically distinct and matched to the respective patient genotypes (data not shown), with no mutations in EGFR recorded. Tumor spheres were established, using the 3 cell lines NCC-HN1, NCC-HN19, and NCC-HN26 (Fig. 1A). These could be propagated as spheres or re-established into monolayer culture, recapitulating the original cell line phenotype. RT-PCR and Western blots showed higher expression of stem cell markers KLF4, SOX2, and Nanog in tumor spheres than in monolayer culture cells (Fig. 1B), indicating a higher stem cell fraction when these cell lines are grown as tumor spheres.

### HNSCC Tumor Spheres Are Resistant to Chemotherapy and Radiation

To determine the response of cells grown as tumor spheres to chemotherapy and radiation, the NCC-HN1 and NCC-HN19 cell lines were treated with $\gamma$-radiation, 5-FU, cisplatin, and etoposide, which are commonly used in the treatment of patients with HNSCC. Apoptotic fractions were obtained 48 hours after treatment for cell lines grown as tumor spheres or monolayer culture and showed that cells grown as tumor spheres were more resistant to all four treatment regimens than cells grown in monolayer culture (Fig. 1C).

### ALD+ Cells Are Concentrated in Tumor Spheres and Exhibit Stem Cell Phenotype

Previous data have shown that CD44 is not a useful marker to isolate CSCs in HNSCC cultures because the cells uniformly express this surface marker. Our own studies indicate that with serial passaging of primary tumors, CD44 gradually increases and is universally expressed by all cells after 6–12 passages (data not shown). In contrast, ALD activity based on the ALDEFLUOR assay is able to separate the lines into two distinct subpopulations and has been shown in a number of studies to be higher in CSCs [7, 13]. Our own clinical data show that ALDEFLUOR-positive (ALD+) fractions showed a range in primary tumors and that high fractions were associated with higher recurrence and mortality rates (unpublished data). ALD+ fractions were determined in NCC-HN1, NCC-HN19, and NCC-HN26 cell lines grown as monolayer culture or tumor spheres. Flow cytometry showed that ALD+ fractions were consistently higher in tumor spheres than in monolayer culture (Fig. 2A). NCC-HN1 and NCC-HN19 cell lines were serially propagated in spheroid cultures as secondary and tertiary spheres, each derived from the respective preceding sphere passage, and the ALD+ fractions were determined. Serial propagation showed a reduction in the size of the spheres but the ALD+ fraction was increased in each of the spheres with each passage. High ALD+ fractions were maintained even when cells from the tertiary spheres were plated as monolayer cultures (Fig. 2B). This increase in ALD+ fractions correlated with an increase in stem cell markers, demonstrating that these techniques were concentrating a CSC subpopulation rather than merely increasing ALD activity (data not shown). We sought to determine whether the concentration of ALD+ cells per stem cell fraction resulted from phenotypic selection in cells grown as spheres or was secondary to the growth factors in the spheroid media. The growth factors used in spheroid media (insulin, EGF, and bFGF) were added to monolayer cultures of NCC-HN1, NCC-HN19, and NCC-HN26, and the ALD+ fractions were determined. The addition of EGF and/or insulin was sufficient to increase ALD+ to the same levels seen in the second and third generation tumor spheres, suggesting that the growth factors in which the cells were maintained were responsible for concentrating the ALD+ cells (Fig. 2C).

### ALD+ Clones Demonstrate Features of CSCs Suggestive of EMT

In order to examine the dynamics of the ALD+ and ALD− cellular subpopulations, we sought to establish a cell line based model for each of these states. To do this, NCC-HN1, NCC-HN19, and NCC-HN26 monolayer cultures were subject to single cell cloning by serial dilution to generate clones with high and low ALD+ fractions. ALDEFLUOR fractions were obtained 2 weeks after clonal selection, and Table 2 shows the range of ALD+ fractions for the three cell lines. From these, we selected the two clones with the highest ($ALD^{High}$) and two clones with the lowest ($ALD^{Low}$) ALD+ fractions in each cell line for the subsequent experiments. As hypothesized, $ALD^{High}$ clones showed higher expression of stem cell markers Oct-4, Bmi1, and Nanog compared with $ALD^{Low}$ clones (Fig. 3A). $ALD^{High}$ clones also demonstrated higher clonogenic capacity in vitro compared with $ALD^{Low}$ clones using in vitro colony forming assays by monolayer culture (Fig. 3B, 3C). Moreover, Western blots revealed an expression profile consistent with EMT (Fig. 3D). Apoptosis assays showed that $ALD^{High}$ clones are more resistant to treatment with cytotoxic drugs and radiation compared with $ALD^{Low}$ clones, in a similar fashion to tumor spheres (Fig. 3E). Colony forming assays were subsequently performed as a surrogate for cell survival, and these confirmed the above findings, showing $ALD^{High}$ clones to be more resistant to cytotoxic chemotherapeutic drugs and ionizing radiation in sharp contrast to $ALD^{Low}$ clones (Fig. 3F).

### ALD+ Cells Are Dynamic Subpopulation of Cells and Are Dependent on IGF and EGF

Having shown that growth factor stimulation was sufficient for increasing ALD+ fractions, we then asked whether this was secondary to self-renewal of ALD+ CSCs or conversion of ALD− cells to ALD+ cells. $ALD^{High}$ clones from NCC-HN1, NCC-HN19, and NCC-HN26 were cultured over time to document the ALD+

 

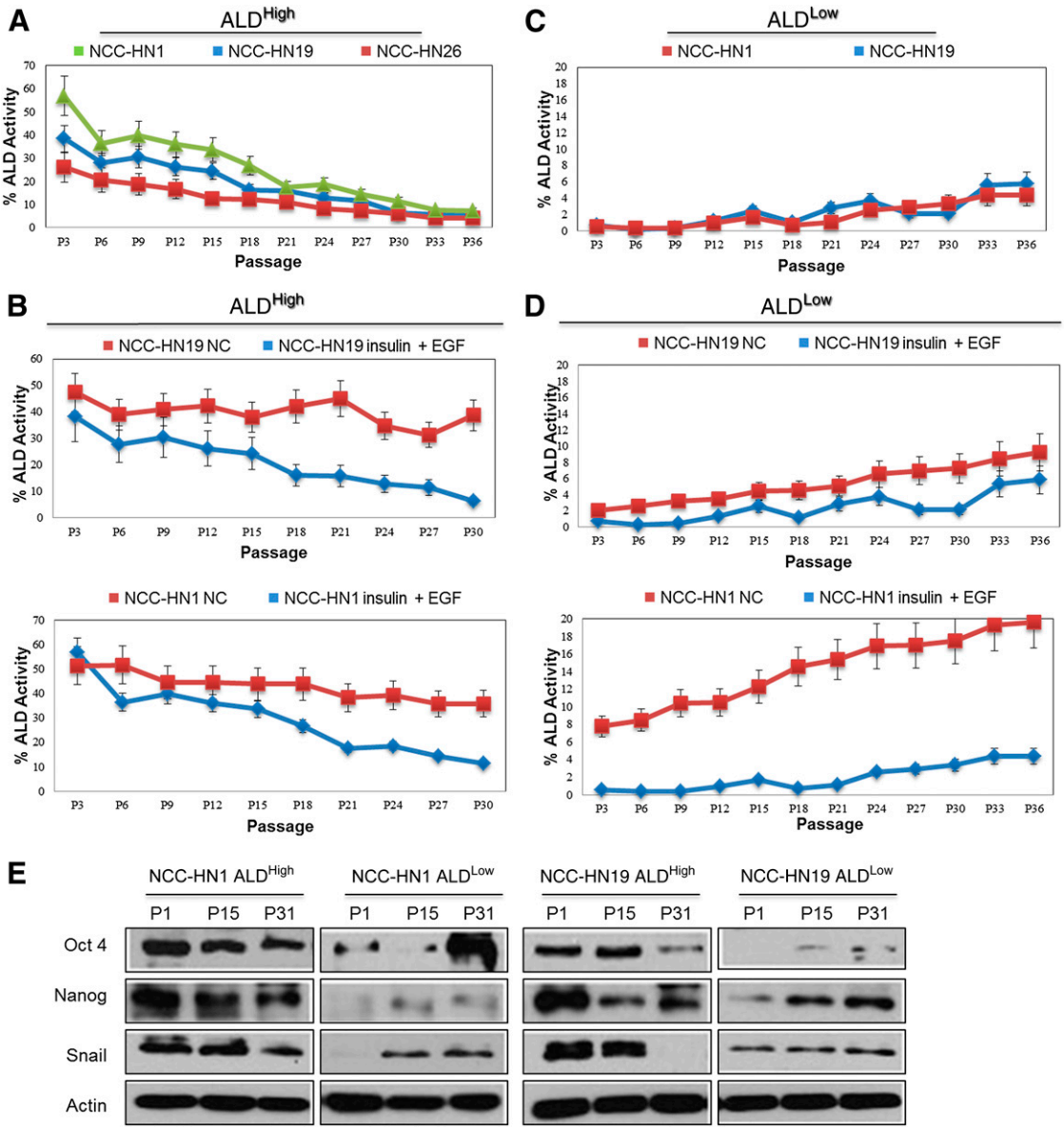


**Figure 4.** ALD+ cellular fractions demonstrate phenotypic plasticity and are dependent on IGF1R and EGFR pathways. Graph showing ALD+ fractions where: **(A):** $ALD^{High}$ cells were passaged in normal media. ALD+ fractions reduced gradually over time in culture, and reached baseline ALD+ level, NCC-HN19 (5.5%±SD 0.15), NCC-HN26 (4.1%±SD 0.06) and NCC-HN1 (7.3%±SD 0.06), after 30-36 passages. **(B):** $ALD^{High}$ cells from NCC-HN19 (top) and NCC-HN1 (bottom) were passaged in high EGF and IGF-containing media. ALD+ fractions were maintained at higher levels as compared to untreated cultures. **(C):** $ALD^{Low}$ cells were passaged in normal media. ALD+ fractions increased gradually over time and reached baseline levels: NCC-HN19 (5.8%±SD 0.20) and NCC-HN1 (4.4%±SD 0.06), after 30-36 passages. **(D):** $ALD^{Low}$ cells from NCC-HN19 (top) and NCC-HN1 (bottom) were passaged in high EGF and IGF-containing media. ALD+ fractions were maintained at higher levels as compared to untreated cultures. **(E):** Western blots showing variation in stem cell markers (Oct4, Nanog) and EMT marker (Snail) with ALD+ fractions during passaging of $ALD^{High}$ and $ALD^{Low}$ clones, where the level of these markers correlate with ALD+ levels. ALD+ fractions were determined every three passages by flow cytometry. All experiments were performed in triplicates on the following clones: $ALD^{High}$ cells: NCC-HN1 Clone 24, NCC-HN19 Clone 39, and NCC-HN26 Clone 79 and $ALD^{Low}$ cells NCC-HN1 Clone 33, NCC-HN19 Clone 43, and NCC-HN26 Clone 56 were used. Average values were shown with standard deviation from three independent experiments as indicated. Note that the scale used in each graph differ to demonstrate the impact in greater detail. Western blots were also performed on the same clones as those used for the serial passaging. Abbreviations: ALD, aldehyde dehydrogenase; $ALD^{High}$, clones with high ALD+ fraction; $ALD^{Low}$, clones with low ALD+ fraction; EGF, epidermal growth factor; P, passage.

fractions with repeated passages in monolayer culture (repeated in triplicate for each cell line). Serial passaging shows that the ALD+ fractions reduce gradually over time to equilibrate at a specified ALD+ fraction for each cell line grown in regular monolayer culture media (Fig. 4A). From these experiments, the baseline ALD+ fractions were defined as 5.5% ± 0.152%, 4.1% ± 0.06%, and 7.3% ± 0.06% (1 SD in parentheses) for cell lines NCC-HN1, NCC-HN19, and NCC-HN26, respectively. This baseline ALD+ fraction was achieved after 30–36 passages. When the growth factors EGF and/or insulin were added to the media, ALD+ fractions could be sustained at higher levels than at baseline (Fig. 4B). Surprisingly, similar experiments in

 

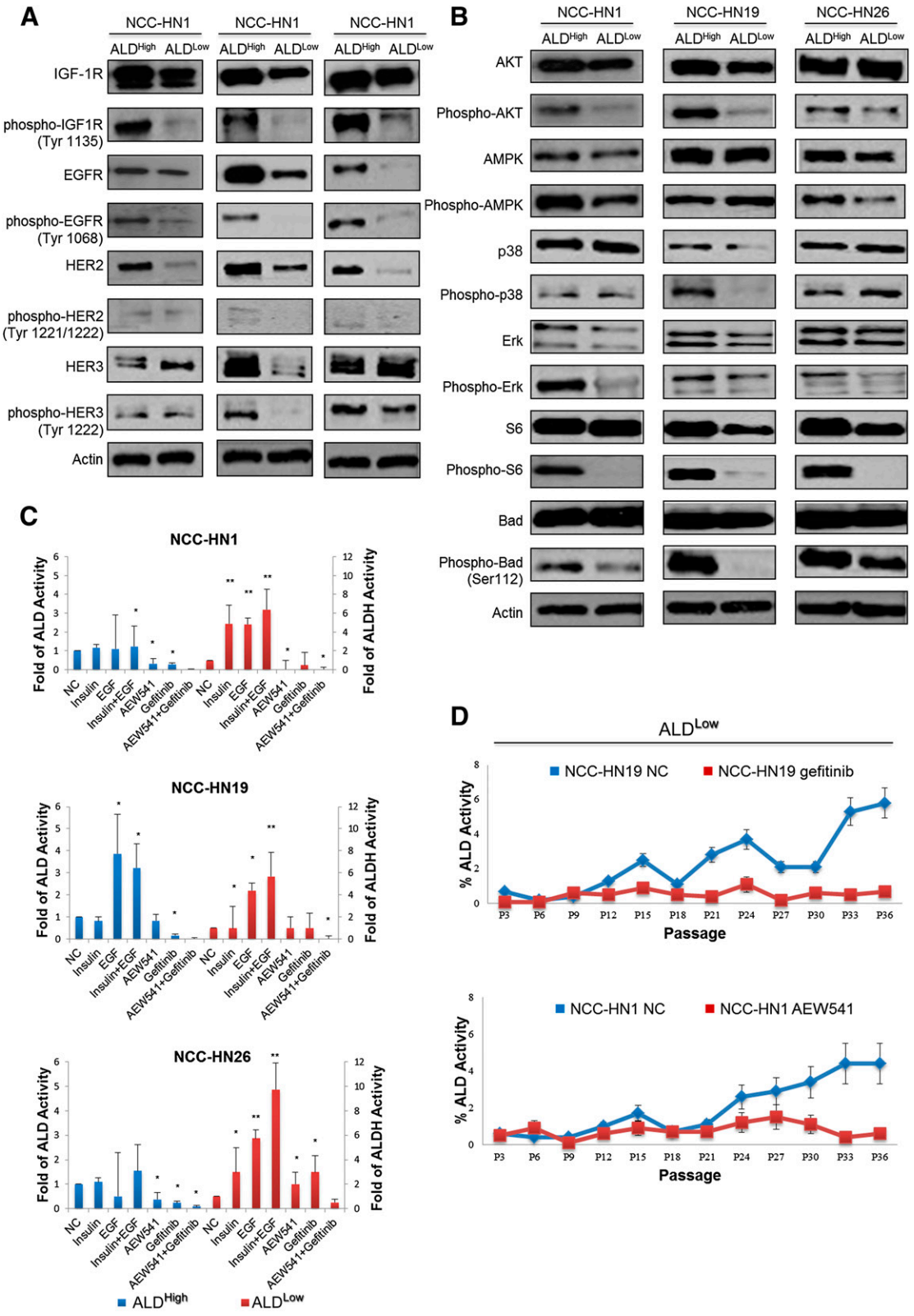


**Figure 5.** IGF and/or EGF addiction underlies the maintenance of ALD+ cellular fractions. Western blots showing activation of EGF-R, IGF-1R, HER2, HER3 (with actin loading control) **(A)** and downstream signal transduction pathway in ALD$^{High}$ cells, particularly PI3K/AKT and ERK signaling (with actin loading control) **(B). (C):** Graph showing ALD+ fractions in ALD$^{High}$ cells treated with Gefitinib and/or AEW541, ALD$^{Low}$ cells after addition of EGF, FGF, and insulin. These demonstrate a significant reduction in ALD+ fractions in ALD$^{High}$ after addition of the drugs and increasing levels of ALD+ cells in ALD$^{Low}$ after addition of growth factors, respectively. ALDEFLUOR assays were performed 3 days after treatment and the ALDH levels were normalized to untreated controls and standard deviation is indicated (*, $p < .05$, **, $p < .01$). **(D):** Graph

(*Figure legend continues on next page*.)

$ALD^{Low}$ clones showed increasing ALD+ fractions with serial passages for all the cell lines examined, equilibrating as similar baseline fractions such as were seen in $ALD^{High}$ clones (Fig. 4C). More importantly, the baseline ALD+ fractions were significantly higher when these cells were grown in media enriched with EGF and insulin (Fig. 4D). For all these experiments, variations in the ALD+ fractions correlated with the expression of stem cell and EMT markers, corroborating that these changes represent variations in stem cell content and not merely a variation in ALD activity (Fig. 4E). In order to validate these results and ensure that this phenomenon was not peculiar to the subclones, we performed the same experiments using cells sorted by FACS into ALD+ and ALD− cell populations. Similar results were obtained with regard to equilibration of ALD+ fractions and the effect of growth factors on the ALD+ and ALD− cell fractions (data not shown). Together, these data suggest that the ALD+ subpopulation is a dynamic cell fraction dependent on EGF and insulin that can be derived from self-renewal of ALD+ cells and reversal or dedifferentiation of ALD− to ALD+ cells, such as seen in the $ALD^{Low}$ clones.

### HNSCC Stem Cells Are Therapeutically Vulnerable to Dual Targeting of IGF-R and EGFR Pathways

Given the dependence on EGF and insulin, we postulated that $ALD^{High}$ clones might have intrinsic activation of the EGFR and either IGF-1R or insulin receptor pathways. Western blots showed that $ALD^{High}$ clones showed increased EGFR and IGF-1R phosphorylation and pathway activation compared with $ALD^{Low}$ clones (but not insulin receptor activation), consistent with their role in the maintenance of the ALD+ phenotype (Fig. 5A, 5B). We further hypothesized that dual inhibition of both pathways could specifically target and reduce the ALD+ fraction. Hence, $ALD^{High}$ clones were treated with the EGFR inhibitor gefitinib and IGF-1R inhibitor AEW 541, individually and in combination. ALDEFLUOR assays showed that although the ALD+ fractions were significantly reduced in the three lines after treatment with the individual inhibitors, maximal reduction was seen after combined treatment with both drugs (Fig. 5C). The absolute effect of each inhibitor was slightly different in each of the cell lines tested, suggesting variability in pathway addiction and drug sensitivity of the ALD+ fraction. Nevertheless, the combined effect of the two inhibitors in all the cell lines was greater than that with the individual drugs. In similar fashion, treatment of $ALD^{Low}$ clones with these inhibitors (either individually or together) circumvented the increase in ALD+ cellular fraction to baseline levels, with a greater effect seen by blocking the pathways that the cell line was more addicted to: in this case, EGFR inhibition for NCC-HN19 and IGF-1R inhibition for NCC-HN1 (Fig. 5D). Taken together, these results validate the crucial role of the EGFR and IGF-1R pathways in maintaining the ALD+ cell fraction, and highlight a potential therapeutic strategy.

## Discussion

Solid tumors are composed of heterogeneous cell subpopulations with differing mutations, expression patterns, and phenotypes. The stem cell hypothesis provides a hierarchy to this heterogeneity, such that a de-differentiated, treatment-resistant subclone has the ability to recapitulate other subpopulations given the appropriate conditions [4, 5]. In this study, we used patient derived cell lines as a preclinical model to evaluate stem cell plasticity as measured by ALDEFLUOR content, an established marker for stem cell phenotype. We confirm that the growth of cells as spheroids select for a ALD+ subpopulation that expressed higher levels of stem cell and EMT markers and exhibited chemotherapy and radiation resistance in vitro. Importantly, the increase in ALD+ fraction is dynamic and dependent on growth factor stimulation and could be circumvented by IGF-1R and EGFR targeting agents.

Our data from single cell clones show that each individual cell lineage equilibrates at a specific ALD+ fraction that is dependent on both intrinsic (cell context) and extrinsic (culture conditions or microenvironment) factors. This equilibrium is reached even in nonstem ALD cells, which demonstrate plasticity and the ability to dedifferentiate into the ALD+ stem-like cell. Indeed, this might be the explanation for previously published data showing that "non-cancer stem cell fractions" (which include experiments using ALD− cells) are still clonogenic and have the ability to reconstitute tumors, albeit at reduced efficiency [13, 14]. Hence, although hematologic malignancies tend to follow a linear hierarchy of differentiation [18], our data suggest that stem-like cell populations can undergo bidirectional transition between differentiation and de-differentiation, consistent with the previously reported Markov modeling of cell state dynamics of luminal, basal, and stem-like breast cancer cell populations [25]. In our model, ALD+ and ALD+ cellular populations demonstrated plasticity, such that CSCs and differentiated tumor cells freely interconvert in a stochastic manner. The concept of a nonrigid hierarchy contends that CSCs can be formed de novo from more differentiated tumor cells. Previous studies and our data posit that this dynamic model can be influenced by intrinsic factors (e.g., genetic perturbations) and extrinsic factors, including chemotherapy and growth factor milieu [26, 27]. The phenotypic equilibrium of our patient-derived HNSCC cell lines was dependent on growth factors, specifically, activation of the IGF-1R and EGFR pathways, and, importantly, could be manipulated in vitro by growth factor deprivation and inhibition using drugs targeting EGFR or IGF-1R. Combination therapy maximally suppressed the ALD+ fraction in a sustained manner, likely through abrogating the propagation and replenishment of the CSC subpopulation rather than specifically killing the CSCs. These results suggest that the stem cell populations, represented by clones with high ALD fractions, are addicted to these pathways for maintenance of the stem cell phenotype.

(*Figure legend continued from previous page*.)
showing ALD+ fractions where $ALD^{Low}$ cells were cultured with media containing Gefitinib or AEW541. ALD+ fractions did not increase to baseline levels when maintained in drug enriched media, compared to untreated controls. ALD+ fractions were determined every 3 passages by flow cytometry, and all experiments were performed in triplicates and average values were shown. Western blots were performed on clones with the most extreme ALD fractions, so for $ALD^{High}$ cells NCC-HN1 Clone 24, NCC-HN19 Clone 39, and NCC-HN26 Clone 79 were used while for $ALD^{Low}$ cells NCC-HN1 Clone 33, NCC-HN19 Clone 43, and NCC-HN26 Clone 56 were used. For drug assays, two clones per cell line were used as indicated, and each cell line experiment was performed in triplicate, with data showing the average and standard deviation of these. Abbreviations: ALD/ALDH, aldehyde dehydrogenase; $ALD^{High}$, clones with high ALD+ fraction; $ALD^{Low}$, clones with low ALD+ fraction; EGF, epidermal growth factor; EGFR, epidermal growth factor receptor; NC, negative control (untreated).

 

It is noteworthy that monotherapy trials of IGF-1R or EGFR inhibitors in patients with HNSCC have been disappointing to date. In a phase II trial of figitumumab (a monoclonal antibody targeting IGF-1R) in metastatic HNSCC, activation of the EGFR pathway has been suggested to be a potential resistance mechanism [28]. Furthermore, EGFR signaling has been shown to promote stem cell-like properties [29]. Conversely, EGFR inhibition in breast and central nervous system malignancies has been shown to reduce stem cell fractions [28, 30, 31]. In line with our findings, we posit that both EGFR and IGF-1R signaling contributes to the stem cell-like phenotype and that the relative dependency (or "addiction") to either pathway dictates therapeutic vulnerability. Clearly, an intrinsic bias exists to one or the other pathway in the cell line system described, in which NCC-HN19 appears to be more dependent on EGFR and NCC-HN1 to be more addicted to IGF-1R. Notwithstanding, inhibition of the less-addicted pathway (IGF-1R for NCC-HN19 and EGFR for NCC-HN1, respectively) still resulted in additional reduction in the ALD+ fraction, suggesting that a "dose-dependent" addiction is present across parallel growth pathways. Thus, combinatorial approaches to inhibiting IGF-1R and EGFR can abrogate the process of self-renewal and de novo conversion of differentiated cells to CSCs—and might represent a viable therapeutic strategy [32]. Nevertheless, it is prudent to note that these experiments have not explored the contribution of other growth factor pathways involving FGF receptor and platelet-derived growth factor receptor to the maintenance of the stem cell phenotype. Similarly, they do not dictate that the ligand involved in these situations is necessarily EGF and/or IGF-1, because a range of ligands are able to activate these pathways in vivo.

One drawback is the relevance of such in vitro experiments in a field dominated by xenograft experiments. Isolating stem-like cells using ALDEFLUOR or tumor sphere growth are well-established cell culture techniques validated in a range of cancers, including HNSCC [7, 13, 17]. More importantly, a recent publication using an in vivo triple-negative breast cancer mouse model showed that tumor plasticity, specifically with regard to the metastatic phenotype, is dependent on EGF and IGF-1 levels in the tumor microenvironment [33]. High expression of EGF and IGF-1 was shown to enhance the expression of factors associated with stemness and EMT. Despite the contrasting approach (in vivo mouse model breast cancer vs. purely in vitro HNSCC), the conclusion of that study and ours (respectively) emphasize the importance of combinatorial therapy with EGFR and IGF-1R inhibitors to prevent malignant progression. Additional studies are ongoing to examine whether cell viability is significantly increased with manipulation of stem cell-like fraction, and whether additional synergy results with the combination of chemotherapy.

## Conclusion

We have shown that stem cell subpopulations exist in a dynamic equilibrium that depends on both cellular context and the microenvironment. Of interest, growth factors (e.g., IGF and EGF) can augment the stem cell phenotype and can be targeted with IGF-1R and EGFR pathway inhibitors. The latter has important implications from a therapeutic viewpoint, because targeting the pathways responsible for repopulating and/or maintaining the "stem cell population," might pave the way for novel combinatorial treatment strategies to overcome drug resistance in HNSCC.

## Acknowledgments

N.G.I. is supported by a National Medical Research Council (Singapore) clinician-scientist award. Further support for this project was obtained from National Medical Research Council Grant 1209/2009.

## Author Contributions

H.S.L.: conception and design, collection and/or assembly of data, data analysis and interpretation, manuscript writing; F.T.C., P.H.S., D.P.L., and B.H.W.: collection and/or assembly of data; B.-T.T.: provision of study material or patients, data analysis and interpretation; D.S.W.T. and N.G.I.: conception and design, data analysis and interpretation, manuscript writing, financial support, final approval of manuscript.

## Disclosure of Potential Conflicts of Interest

D.S.W.T. is a compensated consultant for Bayer and Novartis and has compensated research funding from Novartis.

## References

1 Hammerman PS, Jänne PA, Johnson BE. Resistance to epidermal growth factor receptor tyrosine kinase inhibitors in non-small cell lung cancer. Clin Cancer Res 2009;15:7502–7509.

2 Ferlay J, Shin H, Bray F et al. Estimates of worldwide burden of cancer in 2008: GLOBOCAN 2008. Int J Cancer 2010;127:2893–2917.

3 Vermorken JB, Specenier P. Optimal treatment for recurrent/metastatic head and neck cancer. Ann Oncol 2010;21(suppl 7):vii252–vii261.

4 Medema JP. Cancer stem cells: the challenges ahead. Nat Cell Biol 2013;15:338–344.

5 Wicha MS, Liu S, Dontu G. Cancer stem cells: An old idea—A paradigm shift. Cancer Res 2006;66:1883–1890.

6 Pardal R, Clarke MF, Morrison SJ. Applying the principles of stem-cell biology to cancer. Nat Rev Cancer 2003;3:895–902.

7 Ginestier C, Hur MH, Charafe-Jauffret E et al. ALDH1 is a marker of normal and malignant human mammary stem cells and a predictor of poor clinical outcome. Cell Stem Cell 2007;1:555–567.

8 Chen C, Wei Y, Hummel M et al. Evidence for epithelial-mesenchymal transition in cancer stem cells of head and neck squamous cell carcinoma. PLoS One 2011;6:e16466.

9 Zhang P, Zhang Y, Mao L et al. Side population in oral squamous cell carcinoma possesses tumor stem cell phenotypes. Cancer Lett 2009;277:227–234.

10 Zhang WC, Shyh-Chang N, Yang H et al. Glycine decarboxylase activity drives non-small cell lung cancer tumor-initiating cells and tumorigenesis. Cell 2012;148:259–272.

11 Song J, Chang I, Chen Z et al. Characterization of side populations in HNSCC: Highly invasive, chemoresistant and abnormal Wnt signaling. PLoS One 2010;5:e11456.

12 Zhou S, Schuetz JD, Bunting KD et al. The ABC transporter Bcrp1/ABCG2 is expressed in a wide variety of stem cells and is a molecular determinant of the side-population phenotype. Nat Med 2001;7:1028–1034.

13 Clay MR, Tabor M, Owen JH et al. Single-marker identification of head and neck squamous cell carcinoma cancer stem cells with aldehyde dehydrogenase. Head Neck 2010;32:1195–1201.

14 Prince ME, Sivanandan R, Kaczorowski A et al. Identification of a subpopulation of cells with cancer stem cell properties in head and neck squamous cell carcinoma. Proc Natl Acad Sci USA 2007;104:973–978.

15 Joshua B, Kaplan MJ, Doweck I et al. Frequency of cells expressing CD44, a head and neck cancer stem cell marker: Correlation with tumor aggressiveness. Head Neck 2012;34:42–49.

16 Tsang JY, Huang YH, Luo MH et al. Cancer stem cell markers are associated with adverse biomarker profiles and molecular subtypes of breast cancer. Breast Cancer Res Treat 2012;136:407–417.

**17** Charafe-Jauffret E, Ginestier C, Iovino F et al. Aldehyde dehydrogenase 1-positive cancer stem cells mediate metastasis and poor clinical outcome in inflammatory breast cancer. Clin Cancer Res 2010;16:45–55.

**18** Bonnet D, Dick JE. Human acute myeloid leukemia is organized as a hierarchy that originates from a primitive hematopoietic cell. Nat Med 1997;3:730–737.

**19** Kai K, Nagano O, Sugihara E et al. Maintenance of HCT116 colon cancer cell line conforms to a stochastic model but not a cancer stem cell model. Cancer Sci 2009;100: 2275–2282.

**20** Gupta PB, Fillmore CM, Jiang G et al. Stochastic state transitions give rise to phenotypic equilibrium in populations of cancer cells. Cell 2011;146:633–644.

**21** Scheel C, Eaton EN, Li SH et al. Paracrine and autocrine signals induce and maintain mesenchymal and stem cell states in the breast. Cell 2011;145:926–940.

**22** Liu S, Dontu G, Mantle ID et al. Hedgehog signaling and Bmi-1 regulate self-renewal of normal and malignant human mammary stem cells. Cancer Res 2006;66:6063–6071.

**23** Vermeulen L, De Sousa E Melo F, van der Heijden M et al. Wnt activity defines colon cancer stem cells and is regulated by the microenvironment. Nat Cell Biol 2010;12:468–476.

**24** Zhao Y, Hamza MS, Leong HS et al. Kruppel-like factor 5 modulates p53-independent apoptosis through Pim1 survival kinase in cancer cells. Oncogene 2008;27:1–8.

**25** Gupta PB, Fillmore CM, Jiang G et al. Stochastic state transitions give rise to phenotypic equilibrium in populations of cancer cells. Cell 2011;146:633–644.

**26** Shestopalov IA, Zon LI. Stem cells: The right neighbour. Nature 2012;481:453–455.

**27** Medema JP, Vermeulen L. Microenvironmental regulation of stem cells in intestinal homeostasis and cancer. Nature 2011;474: 318–326.

**28** Schmitz S, Kaminsky-Forrett M, Henry S et al. Phase II study of figitumumab in patients with recurrent and/or metastatic squamous cell carcinoma of the head and neck: Clinical activity and molecular response (GORTEC 2008-02). Ann Oncol 2012;23:2153–2161.

**29** Abhold EL, Kiang A, Rahimy E et al. EGFR kinase promotes acquisition of stem cell-like properties: A potential therapeutic target in head and neck squamous cell carcinoma stem cells. PLoS One 2012;7:e32459.

**30** Griffero F, Daga A, Marubbi D et al. Different response of human glioma tumor-initiating cells to epidermal growth factor receptor kinase inhibitors. J Biol Chem 2009;284:7138–7148.

**31** Del Vecchio CA, Jensen KC, Nitta RT et al. Epidermal growth factor receptor variant III contributes to cancer stem cell phenotypes in invasive breast carcinoma2012;72:2657–2671.

**32** Molina-Peña R, Álvarez MM. A simple mathematical model based on the cancer stem cell hypothesis suggests kinetic commonalities in solid tumor growth. PLoS One 2012;7: e26233.

**33** Castaño Z, Marsh T, Tadipatri R et al. Stromal EGF and IGF1 together modulate plasticity of disseminated triple negative breast tumors. Cancer Discov 2013;8:922–935.

 